

Gap Anisotropy and de Haas-van Alphen Effect in Type-II Superconductors

Kouji Yasui and Takafumi Kita

Physikalisches Institut, Universität Bayreuth, 95440 Bayreuth, Germany
and

Division of Physics, Hokkaido University, Sapporo 060-0810, Japan
(December 2, 2024)

We present a theoretical study on the de Haas-van Alphen (dHvA) oscillation in the vortex state of type-II superconductors, with a special focus on the connection between the gap anisotropy and the oscillation damping. Numerical calculations for three different gap structures clearly indicate that the average gap along extremal orbits is relevant for the magnitude of the extra damping, thereby providing a support for experimental efforts to probe gap anisotropy through the dHvA signal. We also derive an analytic formula for the extra damping which gives a good fit to the numerical results.

A bouncing number of materials have been found in the 1990's to exhibit the de Haas-van Alphen (dHvA) oscillation in the superconducting vortex state [1], the phenomenon discovered by Graebner and Robbins in 2H-NbSe₂ [2]. Many theories have been put forward during the same period to explain this fundamental phenomenon observed in the system without a well-defined Fermi surface [1]. However, there still exists no established theory comparable with the normal-state Lifshitz-Kosevich (LK) one [3]. Moreover, what is lacking seems a clear physical picture for the mechanism of the extra oscillation damping in the vortex state.

To improve the situation, we here present a numerical study combined with an analytical one. Since the data from real materials may contain complicated unknown effects, numerical results based on a well-defined model will be helpful to obtain an established formula. Hence those numerical results will be used here for a critical evaluation of the theories proposed so far. On the other hand, the aim of our analytic study is to provide a formula to reproduce the numerical results which simultaneously contains a clear-cut picture on the damping mechanism. During the course of the study, we will also focus on the issue raised by Miyake [4], i.e. the connection between the extra damping and the gap anisotropy. The motivation comes from the experiment by Terashima *et al.* on YNi₂B₂C where the oscillation is seen to persist down to a surprisingly low field of order $0.2H_{c2}$ [5]. On the other hand, a specific-heat experiment at $H=0$ shows a power-law behavior $\propto T^3$ at low temperatures [6], indicating an existence of the gap anisotropy in this material. This gap anisotropy may also play an important role for the dHvA signal far below H_{c2} .

It should be noted that numerical studies have already been performed for the isotropic s -wave model [7]. However, they are two-dimensional calculations on the continuum model with the quadratic dispersion, which may fail to describe real three-dimensional materials. First of all, the dHvA effect of the vortex state in three dimensions may be quantitatively different from that in

two dimensions, as may be seen from the presence of the extra phase $\pm\pi/4$ in the expression of the normal-state magnetization. Second, self-consistent calculations for the continuum model necessarily results in a rather small number of Landau levels below the Fermi energy ε_F , i.e. $N_F \sim 10$ at H_{c2} , hence failing to meet the condition $N_F \gg 1$ appropriate for real materials. Notice that $N_F \gg 1$ is also a basic assumption in deriving the LK formula. With these observations, we perform three-dimensional calculations with much more Landau levels below ε_F , i.e. $N_F \sim 50$ for the extremal orbit at H_{c2} .

Another point to be mentioned is a discrepancy between the experiments and the microscopic mean-field theory of the vortex states. According to the theory [7–9], the dHvA oscillation in the vortex state should be accompanied by an oscillatory reentrant behavior of H_{c2} , which cannot be washed out by impurities dilute enough for the dHvA effect to be observable. Such a singular behavior of H_{c2} (i.e. the pair potential), however, has never been identified definitely in any materials displaying the dHvA oscillation in the vortex state. This fact seems to indicate that one should use the quasiclassical pair potential without the oscillatory behavior rather than the fully self-consistent one. Hence we will adopt the former, leaving the puzzling discrepancy for a future resolution. Notice in addition that the use of the quasiclassical pair potential may be completely justified to investigate the persistence of the oscillation at low magnetic fields.

Model: Our starting point is the Bogoliubov-de Gennes equation for the quasiparticle wavefunctions \mathbf{u}_s and \mathbf{v}_s^* labeled by a quantum number s with $E_s > 0$:

$$\int d\mathbf{r}_2 \begin{bmatrix} \underline{\mathcal{H}}(\mathbf{r}_1, \mathbf{r}_2) & \underline{\Delta}(\mathbf{r}_1, \mathbf{r}_2) \\ -\underline{\Delta}^*(\mathbf{r}_1, \mathbf{r}_2) & -\underline{\mathcal{H}}^*(\mathbf{r}_1, \mathbf{r}_2) \end{bmatrix} \begin{bmatrix} \mathbf{u}_s(\mathbf{r}_2) \\ -\mathbf{v}_s^*(\mathbf{r}_2) \end{bmatrix} = E_s \begin{bmatrix} \mathbf{u}_s(\mathbf{r}_1) \\ -\mathbf{v}_s^*(\mathbf{r}_1) \end{bmatrix}. \quad (1)$$

Here $\underline{\Delta}$ is the pair potential and $\underline{\mathcal{H}}$ denotes the normal-state Hamiltonian in the external field $\mathbf{H} \parallel \hat{\mathbf{z}}$; both are 2×2 matrices to describe the spin degrees of freedom.

We adopt as \mathcal{H} the free-particle Hamiltonian. As for the pair potential, we wish to consider the three cases to yield the following energy gaps at $H=0$:

$$\Delta_{\mathbf{p}} = \begin{cases} \Delta_0 W_p i\sigma_y \\ \Delta_0 W_p \sin^2 \theta_{\mathbf{p}} \cos 2\varphi_{\mathbf{p}} i\sigma_y \\ \Delta_0 W_p \cos \theta_{\mathbf{p}} i\sigma_z \sigma_y \end{cases}, \quad (2)$$

where \mathbf{p} is the momentum, W_p denotes some cut-off function with $W_{p_F}=1$ (p_F : Fermi momentum), $\theta_{\mathbf{p}}$ ($\varphi_{\mathbf{p}}$) is the polar (azimuthal) angle, and σ_j 's are the Pauli matrices. The first one is the isotropic s -wave state, whereas the latter two have four point nodes (d -wave) and a line node (p -wave) in the xy plane, respectively. It then turns out that the orbital part of the corresponding pair potentials in finite fields can be expanded with respect to $\mathbf{r} \equiv \mathbf{r}_1 - \mathbf{r}_2$ and $\mathbf{R} \equiv \frac{1}{2}(\mathbf{r}_1 + \mathbf{r}_2)$ as [10]

$$\Delta(\mathbf{r}_1, \mathbf{r}_2) = \frac{\mathcal{N}_f}{\sqrt{2}} \sum_{N_c} \tilde{\Delta}^{(N_c)}(B) \psi_{N_c \mathbf{q}}^{(c)}(\mathbf{R}_{\perp}) \sum_{N_r m p_z} (-1)^{N_r} \times \psi_{N_r m}^{(r)}(\mathbf{r}_{\perp}) \frac{e^{ip_z z}}{L_z} \times \begin{cases} W_p \\ \frac{1}{2} W_p \sin^2 \theta_{\mathbf{p}} \\ W_p \cos \theta_{\mathbf{p}} \end{cases}. \quad (3)$$

Here N_c and N_r denote the Landau levels in the average flux density B , \mathbf{q} is an arbitrary chosen center-of-mass magnetic Bloch vector, and m signifies the relative angular momentum along the z axis so that $m=0, 0$, and ± 2 for the three cases, respectively, in a system with $\mathcal{N}_f^2/2$ flux quanta and the length L_z along the z axis. The arguments \mathbf{r}_{\perp} and \mathbf{R}_{\perp} denote the (x, y) components, and p and $\theta_{\mathbf{p}}$ are to be evaluated at $p = (p_z^2 + \hbar^2 N_r / l_B^2)^{1/2}$ and $\theta_{\mathbf{p}} = \tan^{-1} \frac{\hbar \sqrt{N_r} / l_B}{p_z}$ with $l_B \equiv (\hbar c / eB)^{1/2}$. See ref. [10] for the expressions of the basisfunctions $\psi_{N_c \mathbf{q}}^{(c)}$ and $\psi_{N_r m}^{(r)}$.

A great advantage of Eq. (3) is that the coefficients $\{\tilde{\Delta}^{(N_c)}\}_{N_c=0}^{\infty}$ completely specify the pair potentials, and the first few terms suffice to describe those of $B \gtrsim 0.1 H_{c2}$ [9,11]. As rationalized earlier, we here adopt the quasi-classical $\tilde{\Delta}^{(N_c)}$ rather than the fully self-consistent one, with the square-root behavior

$$\tilde{\Delta}^{(0)} = a(1 - B/H_{c2})^{1/2} \quad (4)$$

of the mean-field second-order transition for the dominant $N_c = 0$ level. Then the best choice would be to use the results from the Eilenberger equations. Since our main interest lies in studying the differences in the oscillation damping among various gap structures, however, we here adopt a model form of $\tilde{\Delta}^{(N_c)}$ determined by requiring that the maximum of $\frac{1}{V} \int d\mathbf{R} |\int d\mathbf{r} \Delta(\mathbf{r}_1, \mathbf{r}_2) e^{-i\mathbf{p} \cdot \mathbf{r} / \hbar}|^2$ be equal to $\Delta_0^2(1 - B/H_{c2})$, where V is the volume of the system and Δ_0 denotes the maximum energy gap of the weak-coupling theory at $T=H=0$. This is possible within the lowest-Landau-level approximation of retaining only $\tilde{\Delta}^{(0)}$, which is excellent for $B \gtrsim 0.1 H_{c2}$ [9,11]. The resulting $\tilde{\Delta}^{(0)}$ also carries the square-root behavior,

and our numerical calculation shows that $a^2 \approx 0.5 \Delta_0^2$ in all the three cases. We are planning to report on the best choice for a from the Eilenberger equations.

Since the relevant materials have large Ginzburg-Landau parameter $\kappa \gg 1$, we also neglect the screening in the magnetic field. Indeed, the effect has been shown to be irrelevant for the oscillation damping [1]. We put $T=0$, adopt $W_p = e^{-(\xi_p/0.1\varepsilon_F)^4}$ with ξ_p the normal-state one-particle energy measured from ε_F , and choose the cyclotron energy at H_{c2} as $\hbar\omega_{c2} = k_B T_c$, in accordance with $\hbar\omega_{c2}/k_B T_c = 1 \sim 3$ for the real materials.

Numerical Method: To solve it numerically for the above model, we transform Eq. (1) into the eigenvalue problem for the expansion coefficients of \mathbf{u}_s and \mathbf{v}_s in the quasiparticle basisfunctions $\{\psi_{N\mathbf{k}\alpha}\}$, where \mathbf{k} is a quasiparticle magnetic Bloch vector and $\alpha (= 1, 2)$ signifies two-fold degeneracy of the orbital states [10]. Then it can be solved separately for each (\mathbf{k}, α) due to the translational symmetry of the vortex lattice. The overlap integral between $\psi_{N_c \mathbf{q}}^{(c)}(\mathbf{R}_{\perp}) \psi_{N_r m}^{(r)}(\mathbf{r}_{\perp})$ and $\psi_{N_1 \mathbf{k}_1 \alpha_1}(\mathbf{r}_{1\perp}) \psi_{N_2 \mathbf{k}_2 \alpha_2}(\mathbf{r}_{2\perp})$ vanishes unless $\mathbf{q} = \mathbf{k}_1 + \mathbf{k}_2$ and $\alpha_1 = \alpha_2$ so that the calculations are simplified greatly. The corresponding eigenstate is labeled explicitly by $s = (\nu \mathbf{k} \alpha p_z \sigma)$ with ν (σ) the band (spin) index.

As noted before, the self-consistent calculations with the quadratic dispersion fails to reproduce the experimental situation $N_F \gg 1$, and one is forced to adopt a realistic dispersion [9]. The present calculation with the quasichlassical pair potential is free from such a limitation. We have performed calculations of including about 50 Landau levels below ε_F for the extremal orbit at H_{c2} .

Numerical results: Figure 1(a) presents the oscillation of the s -wave magnetization as compared with the normal-state one. With $\hbar\omega_c = k_B T_c$ at H_{c2} , the oscillation is seen to persist down to a rather low field of $0.6 H_{c2}$, which is somewhat smaller than $0.8 H_{c2}$ where $\hbar\omega_c$ becomes equal to the spatial average of the energy gap: $\Delta_0(1 - B/H_{c2})^{1/2}$. The points with error bars in Fig. 1(b) are the corresponding Dingle plot for the extra damping factor R_s obtained by the numerical differentiation. This extra damping at high fields shows the behavior $\propto 1 - B/H_{c2}$ in the logarithmic scale, but an irregularity sets in around $0.6 H_{c2}$ where the oscillation disappears. We attribute this irregularity to the effect of the bound-state formation in the core region. The lines are the predictions from various theoretical formulas. The Maki formula [12] reproduces the correct functional behavior $\propto 1 - B/H_{c2}$ at high fields, but the prefactor is seen too large. The Norman-MacDonald-Akera (NMA) formula [7], deduced from their two-dimensional self-consistent numerical results with $N_F \sim 10$ at H_{c2} , clearly shows a dependence incompatible with our numerical data. The theory of Dukan and Tešanović [13], which would predict $R_s = 0$ in the clean limit of $T=0$, is also inconsistent with the data. The solid line is from our expression for the extra Dingle temperature:

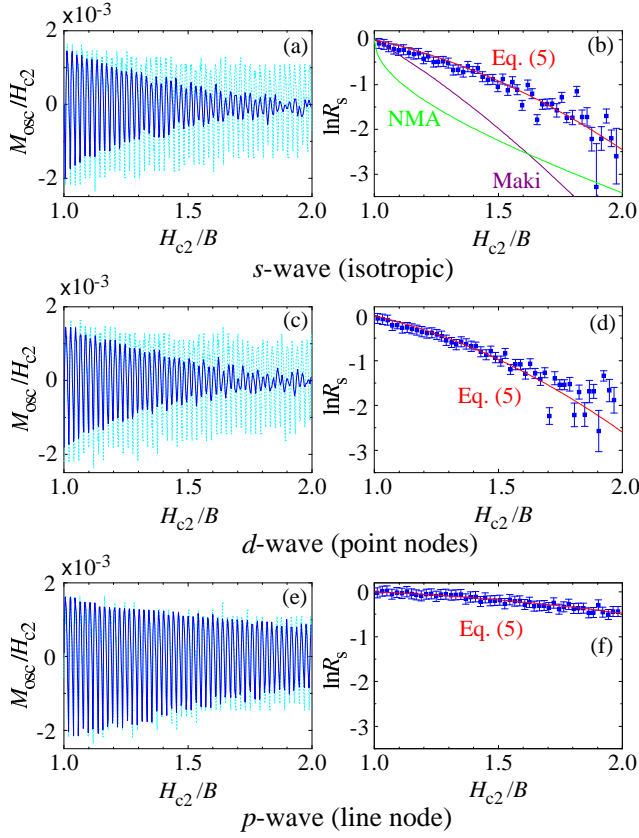


FIG. 1. Left figures: the oscillatory part M_{osc} of the magnetization in the vortex state (full lines) as compared with the normal-state one (dotted lines) for the three cases of Eq. (2). Right figures: the corresponding Dingle plots (points with error bars) compared with theoretical predictions.

$$k_B T_{\Delta} = 0.5 \tilde{\Gamma} \langle |\Delta_{\mathbf{p}}|^2 \rangle_{\text{eo}} \frac{m_b c}{\pi e \hbar} \frac{1 - B/H_{c2}}{B}. \quad (5)$$

Here $\tilde{\Gamma} = 0.125$ is a dimensionless quantity characterizing the Landau-level broadening due to the pair potential, $\langle |\Delta_{\mathbf{p}}|^2 \rangle_{\text{eo}}$ denotes the average energy gap around the extremal orbit in zero field (i.e. Δ_0^2 for the s -wave pairing) and m_b is the band mass. This formula reproduces both the functional dependence and the attenuation magnitude of the numerical data; see below for its derivation.

Figures 1(c)-(d) show the results for the second energy gap in Eq. (2) which vanishes at four points on the Fermi surface along the extremal orbit. The damping is seen to be strong and not much different from the s -wave case. Equation (5) gives a good fit to the numerical data above $0.6 H_{c2}$, thereby indicating that the average gap along the extremal orbit is relevant for the extra damping. Miyake pointed out the possibility of detecting point nodes via the dHvA effect [4], but our data clearly provide a negative answer to it.

In the line-node case of Figs. 1(e)-(f), in contrast, we observe a much weaker damping in favor of Miyake's idea [4]. However, the non-zero extra damping can only be explained by considering the contribution of some finite width near the extremal orbit. Using Eq. (5) to

get the best fit to the numerical data, i.e., solid line of Fig. 1(f), we estimate that the region $|p_z| \lesssim p_F \sin \frac{\pi}{5}$ contributes to the extra attenuation. This is in rough agreement with the estimation from the Fresnel integral $\int_{-\infty}^{\infty} \exp[-i(\sqrt{2\pi N_F} p_z/p_F)^2] dp_z$ which appears in obtaining the LK formula: Cutting the infinite integral at $\sqrt{2\pi N_F} |p_z|/p_F \sim 10$ with $N_F \sim 50$ yields a similar value for the relevant range of p_z .

Analytic Formula: The Luttinger-Ward free-energy functional corresponding to Eq. (1) is given by [14]

$$\Omega = -\frac{k_B T}{2} \sum_n \text{Tr} \ln \begin{bmatrix} \mathcal{H} - i\varepsilon_n \mathbf{1} & \underline{\Delta} \\ -\underline{\Delta}^* & -\mathcal{H}^* - i\varepsilon_n \mathbf{1} \end{bmatrix} \times \begin{bmatrix} e^{i\varepsilon_n 0_+} \mathbf{1} & \underline{0} \\ \underline{0} & e^{-i\varepsilon_n 0_+} \mathbf{1} \end{bmatrix} + \dots, \quad (6)$$

where ε_n/\hbar is the Matsubara frequency and 0_+ is an infinitesimal positive constant. The terms \dots may be expressed solely with respect to the pair potential so that they can be neglected in the present model to consider the oscillatory part. This Ω may be transformed into [14]

$$\Omega = - \sum_s \left[k_B T \ln(1 + e^{-E_s/k_B T}) + E_s \int |\mathbf{v}_s(\mathbf{r})|^2 d\mathbf{r} \right]. \quad (7)$$

Since we are interested in the extra damping in the vortex state, we adopt as E_s and \mathbf{v}_s the expressions from the second-order perturbation with respect to $\underline{\Delta}$. They are

$$E_{N\mathbf{k}\alpha p_z \sigma} = |\xi_{N p_z \sigma}| + \eta_{N\mathbf{k} p_z}^{(1)} \text{sign}(\xi_{N p_z \sigma}), \quad (8)$$

$$\int |\mathbf{v}_{N\mathbf{k}\alpha p_z \sigma}(\mathbf{r})|^2 d\mathbf{r} = \theta(-\xi_{N p_z \sigma}) + \eta_{N\mathbf{k} p_z}^{(2)} \text{sign}(\xi_{N p_z \sigma}), \quad (9)$$

where $\theta(\xi)$ is the step function and $\eta_{N\mathbf{k} p_z}^{(n)} \equiv \sum_{N'} \left| \int \psi_{N\mathbf{k}\alpha}^*(\mathbf{r}_{1\perp}) \psi_{N'\mathbf{q}-\mathbf{k}\alpha}^*(\mathbf{r}_{2\perp}) \frac{e^{-ip_z(z_1-z_2)/\hbar}}{L_z} \Delta(\mathbf{r}_1, \mathbf{r}_2) d\mathbf{r}_1 d\mathbf{r}_2 \right|^2 / (\xi_{N p_z \sigma} + \xi_{N' - p_z - \sigma})^n$. The first terms on the right-hand side of these equations are just the normal-state expressions. The second terms, on the other hand, denote the finite quasiparticle dispersion in the magnetic Brillouin zone and the smearing of the Fermi surface, respectively, due to the scattering by the growing pair potential. It is useful to express $\eta_{N\mathbf{k} p_z}^{(n)}$ in terms of $\tilde{\Delta}^{(0)}(B)$ and the cyclotron energy $\hbar\omega_c$ of the extremal orbit as

$$\eta_{N\mathbf{k} p_z}^{(n)} = \frac{|\tilde{\Delta}^{(0)}(B)|^2}{(\hbar\omega_c)^n} \tilde{\eta}_{N\mathbf{k} p_z}^{(n)}. \quad (10)$$

The quantity $\tilde{\eta}_{N\mathbf{k} p_z}^{(n)}$ thus defined is dimensionless, and one may realize that the main B dependence in Eq. (10) lies in the prefactor $|\tilde{\Delta}^{(0)}(B)|^2/(\hbar\omega_c)^n$. The explicit expression of $\tilde{\eta}_{N\mathbf{k} p_z}^{(n)}$ is given by

$$\tilde{\eta}_{N\mathbf{k} p_z}^{(n)} = \frac{\mathcal{N}_f^2}{4} \sum_{N' m m'} \frac{|\langle N N' | 0 N + N' \rangle|^2 \langle N + N' + m | 2\mathbf{k} - \mathbf{q} \rangle}{[N + N' - 2(N_F + \delta)]^n} \times \langle 2\mathbf{k} - \mathbf{q} | N + N' + m' \rangle \times \begin{cases} 1 \\ \sin^4 \theta_{\mathbf{p}} \\ \cos^2 \theta_{\mathbf{p}} \end{cases}, \quad (11)$$

where the overlap integrals are given by Eqs. (3.23) and (3.29) of ref. [10], $\delta = \delta(B, p_z)$ ($|\delta| < 1/2$) specifies the location of ε_F between the two closest Landau levels, and $m, m' = 0, 0$, and ± 2 for the three cases of Eq. (3), respectively. The corresponding normalized density of states:

$$D_{Np_z}^{(n)}(\tilde{\eta}) \equiv \frac{2}{N_F^2} \sum_{\mathbf{k}\alpha} \delta(\tilde{\eta} - \tilde{\eta}_{N\mathbf{k}p_z}^{(n)}), \quad (12)$$

will play a central role in the following.

Substituting Eqs. (8) and (9) into Eq. (7), we find that the terms containing $\eta_{N\mathbf{k}p_z}^{(2)}$ may be neglected due to the cancellation between the particle and hole contributions. The remaining term can be transformed with the standard procedure. We thereby obtain, for the first harmonic of Ω/V , the expression:

$$\frac{\Omega_1}{V} = -\frac{k_B T}{2\pi^2 l_B^2} \sum_{\sigma} \int_{-1/2}^{\infty} dN \cos(2\pi N) \int_{-\infty}^{\infty} dp_z \int_{-\infty}^{\infty} d\tilde{\eta} \times D_{Np_z}^{(1)}(\tilde{\eta}) \ln[1 + e^{-(\xi_{Np_z\sigma} + \tilde{\eta} |\tilde{\Delta}^{(0)}(B)|^2 / \hbar\omega_c) / k_B T}]. \quad (13)$$

The function $D_{Np_z}^{(1)}(\tilde{\eta})$ depends on (N, p_z) , but may be replaced by a representative one $\overline{D}_{\ell}^{(1)}(\tilde{\eta})$ to be put outside the N and p_z integrals [15], where the recovered index ℓ specifies the s -, d -, or p -wave case of Eq. (11). It may also be permissible to use a Lorentzian for it: $\overline{D}_{\ell}^{(1)}(\tilde{\eta}) = \tilde{\Gamma}_{\ell} / \pi(\tilde{\eta}^2 + \tilde{\Gamma}_{\ell}^2)$ [16]. We thereby obtain an expression for the magnetization which carries an extra damping factor:

$$R_s(B) \equiv \int_{-\infty}^{\infty} \overline{D}_{\ell}^{(1)}(\tilde{\eta}) \exp[-2\pi i \tilde{\eta} |\tilde{\Delta}^{(0)}(B)|^2 / (\hbar\omega_c)^2] d\tilde{\eta} = \exp[-2\pi \tilde{\Gamma}_{\ell} |\tilde{\Delta}^{(0)}(B)|^2 / (\hbar\omega_c)^2]. \quad (14)$$

Thus, the superconductivity gives rise to an extra Dingle temperature of $k_B T_{\Delta} \equiv \tilde{\Gamma}_{\ell} |\tilde{\Delta}^{(0)}(B)|^2 / \pi \hbar\omega_c$, or equivalently, the extra scattering rate of $\tau_s^{-1} \equiv 2\pi k_B T_{\Delta} / \hbar$.

Equation (14) may have an advantage that one can trace the origin of the extra dHvA damping definitely to the growing pair potential, which brings a finite quasiparticle dispersion (11) in the magnetic Brillouin zone and the corresponding Landau-level broadening (12). And Eq. (11) tells us that this broadening near H_{c2} is closely connected with the gap structure (2) at $H=0$.

There seems to be no analytic way of determining $\tilde{\Gamma}_s$, so we fix it by the best fit to the numerical data of Fig. 1(b). Using Eq. (4) with $a^2 = 0.5\Delta_0^2$, the procedure yields $\tilde{\Gamma} \equiv \tilde{\Gamma}_s = 0.125$, as noted before. It is also clear for the anisotropic cases that the average gap around the extremal orbit is relevant for the extra attenuation, as may be realized from Eq. (11). We hence put $a^2 \tilde{\Gamma}_{\ell} = 0.5 \langle |\Delta_{\mathbf{p}}|^2 \rangle_{\text{eo}} \tilde{\Gamma}_s$. We thereby obtain the expression (5), which gives a good fit to the d -wave numerical data without any adjustable parameters; see Fig. 1(d).

Concluding Remarks: We have performed a theoretical study on the dHvA effect in the vortex state to show that the gap anisotropy is detectable by measuring the extra

attenuation of the dHvA oscillation. It should be noted that the numerical factor 0.5 in Eq. (5) comes from our model described below Eq. (4). It has to be replaced by the result from the Eilenberger equations before using Eq. (5) to extract the average gap around the extremal orbits from the dHvA experiments in the vortex state. We are planning to report on it in the near future.

We acknowledge stimulating discussions with Y. Inada and Z. Tešanović. We are also grateful for the hospitality of the members of Institut für Theorie der Kondensierten Materie at Universität Karlsruhe and Physikalisches Institut at Universität Bayreuth, where part of the work has been performed. T.K. is a Yamada Science Foundation overseas research fellow and greatly acknowledges the financial support. Numerical calculations were performed on an Origin 2000 in “Hierarchical matter analyzing system” at the Division of Physics, Graduate School of Science, Hokkaido University.

-
- [1] For a recent review and references, see, T. J. B. M. Janssen, C. Haworth, S. M. Hayden, P. Meeson, and M. Springford, Phys. Rev. B **57**, 11698 (1998).
 - [2] J. E. Graebner and M. Robbins, Phys. Rev. Lett. **36**, 422 (1976).
 - [3] I. M. Lifshitz and A. M. Kosevich, J. Exp. Theor. Phys. **29**, 730 (1955) [Sov. Phys. JETP **2**, 636 (1956)].
 - [4] K. Miyake, Physica B **186-188**, 115 (1993).
 - [5] T. Terashima, C. J. Haworth, H. Takeya, S. Uji, and H. Aoki, Phys. Rev. B **56**, 5120 (1997).
 - [6] R. Movshovich, M. F. Hundley, J. D. Thompson, P. C. Canfield, B. K. Cho, and A. V. Chubukov, Physica C **227**, 381 (1994).
 - [7] M. R. Norman, A. H. MacDonald, and H. Akera, Phys. Rev. B **51**, 5927 (1995).
 - [8] For a review, see, M. Rasolt and Z. Tešanović, Rev. Mod. Phys. **64**, 709 (1992).
 - [9] K. Yasui and T. Kita, unpublished.
 - [10] T. Kita, J. Phys. Soc. Jpn. **67**, 2075 (1998).
 - [11] T. Kita, J. Phys. Soc. Jpn. **67**, 2067 (1998).
 - [12] K. Maki, Phys. Rev. B **44**, 2861 (1991).
 - [13] S. Dukan and Z. Tešanović, Phys. Rev. Lett. **74**, 2311 (1995).
 - [14] T. Kita: J. Phys. Soc. Jpn. **65**, 1355 (1996).
 - [15] The p_z integral in Eq. (13) passes through regions where $\delta \approx 0$ in Eq. (11), i.e. the second-order perturbation is not justified. However, the main contribution to the integral certainly comes from the regions where we can use Eq. (8). Notice that $\delta = -1/8$ at the maximal orbit when the magnetization takes a local maximum.
 - [16] It is found numerically that the variance of Eq. (12) depends little on the values of N_F and N ($\sim N_F$), as expected. It is ~ 0.2 for the s -wave pairing with $\delta = -1/8$.